Electronic Supplementary Information

Exploration of the Intrinsic Factors Limiting Photocurrent Current Density in Ferroelectric $BiFeO_3$ Thin Film

Jafar Hussain Shah[a,b], Hengyun Ye[c] , Yong Liu[a,], Ahmed Mahmoud Idris[a,b], Anum Shahid Malik[a,b], Yi Zhang [c*], Hongxian Han[a,b*], Can Li[a]

[a] State Key Laboratory of Catalysis & Division of Solar Energy, Dalian National Laboratory for Clean Energy, Dalian Institute of Chemical Physics, Chinese Academy of Sciences, Dalian, 116023, China.

[b] University of Chinese Academy of Sciences, Beijing, 100049, China.

[c] Department of Chaotic Matter Science Research Center, Jiangxi University of Science and Technology, Nanchang 330013, P. R. China

Contact author: Prof. Hongxian Han, hxhan@dicp.ac.cn

Corresponding author: Prof. Hongxian Han, hxhan@dicp.ac.cn;

Prof. Yi Zhang, yizhang1980@seu.edu.cn

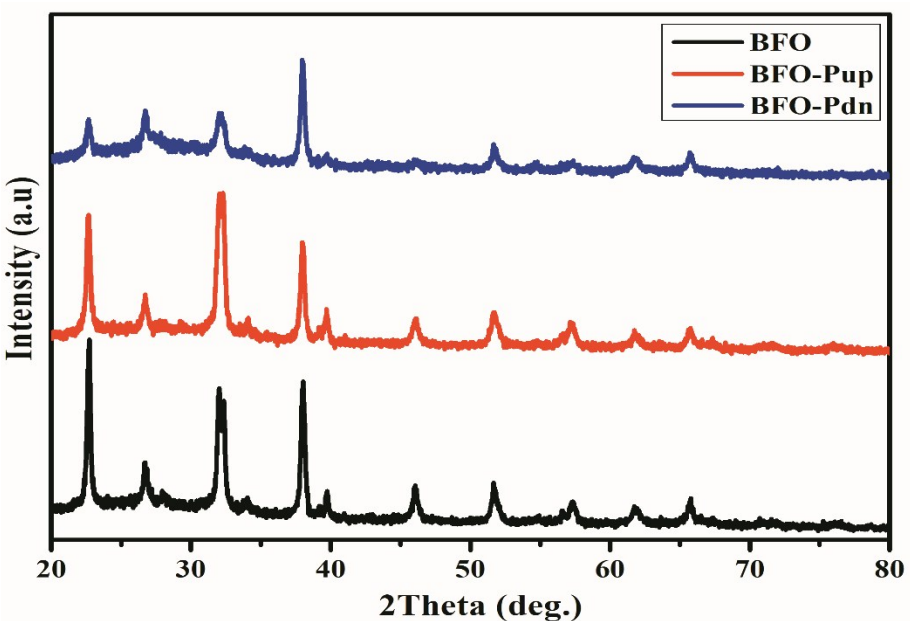

Fig. S1 XRD of BFO-8 before and after polarization.

DFT calculation of density of states

The theoretical bandgap of BFO was also determined by density of states (DOS) calculation using density functional theory (DFT). The electronic configuration of Fe atom is $3d^6 4s^2$. According to the Hund's rules, Fe^{3+} is stabilized by donating two 4s electrons and one 3d electron to facilitate the unpaired electrons of O pairing. This means that the Fe^{3+} in BFO has five unpaired electrons in 3d orbits, therefore, high spin states were set during DFT calculations. As shown in Fig. S2, the CB and VB are mainly contributed by Fe (3d) and O (2p) orbitals, respectively. DOS results also indicate that the spin magnetic moment of BFO is due to Fe atoms as the contribution of the Fe in the up and down DOS is rather different. The bandgap of BFO based on the total DOS is ca. 2.05 eV, which is very close to the value experimentally estimated.

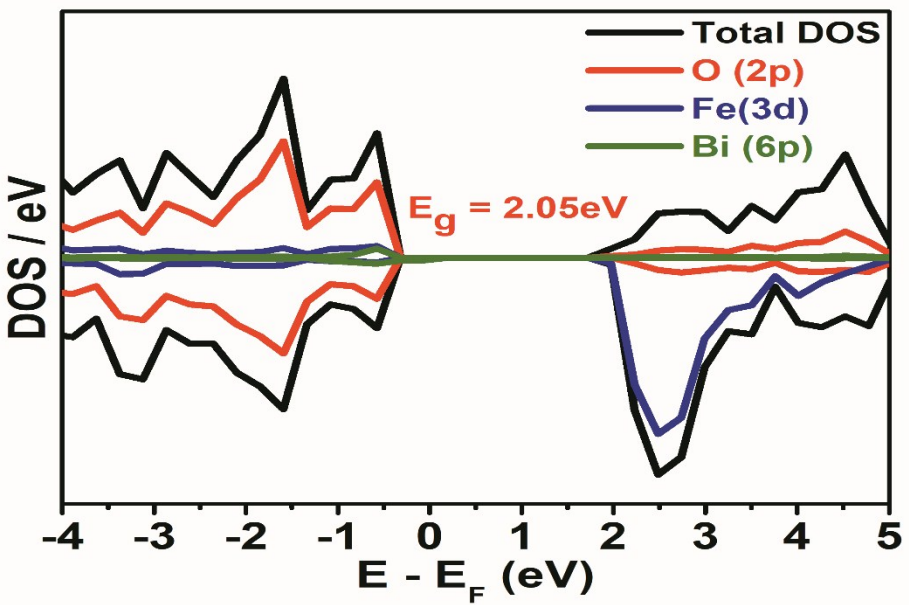

Fig. S2 Total DOS and partial DOS of BFO calculated by DFT calculation.

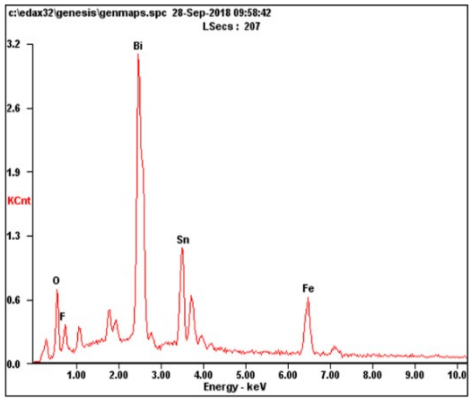

Element	Wt%	At%
OK	12.23	47.56
FK	04.18	13.67
BiM	50.47	15.02
SnL	22.26	11.66
FeK	10.86	12.09
Matrix	Correction	ZAF

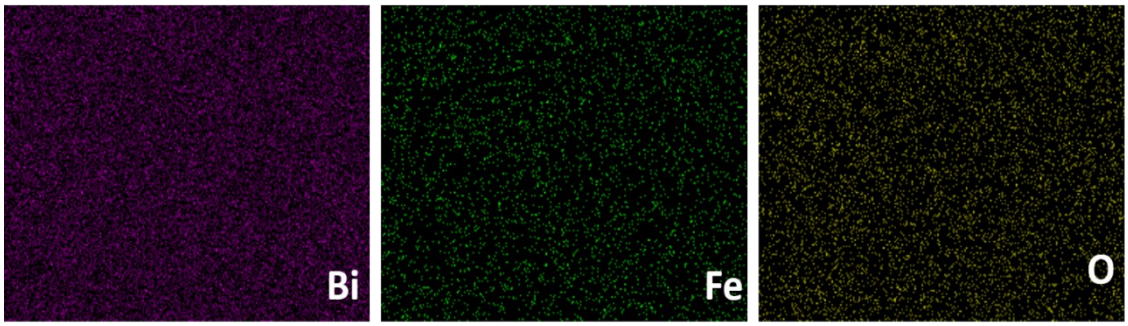

Fig. S3 EDX analysis and elemental mapping of BFO-8

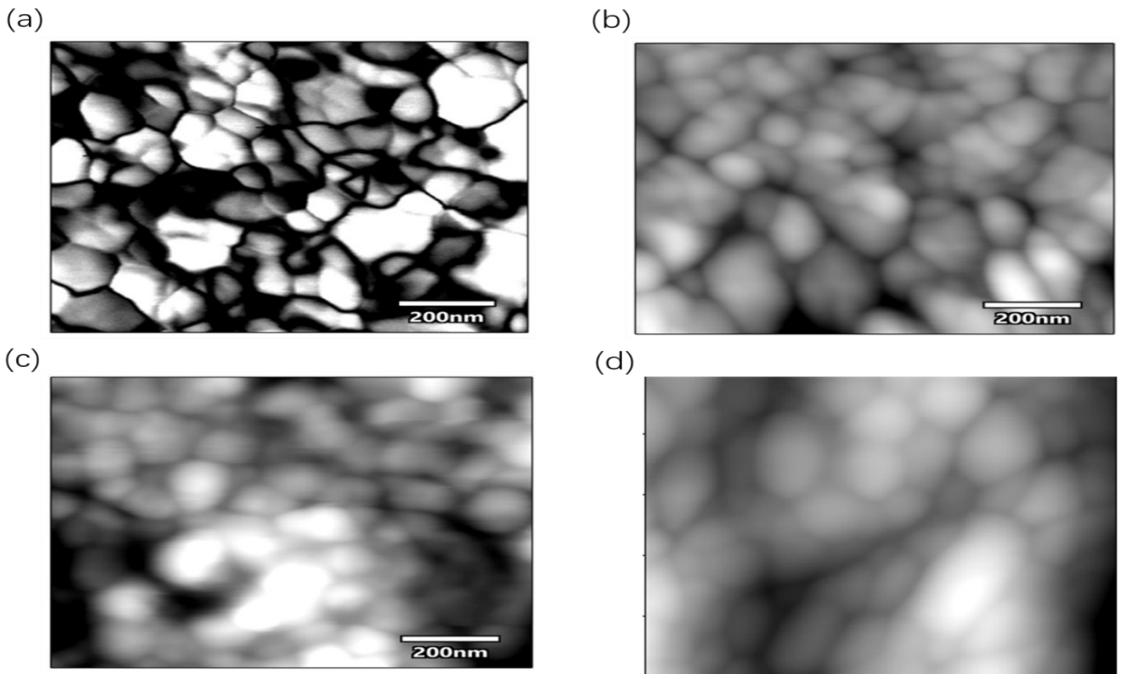

Fig. S4 Film surface images indicating the increase of grain size with increasing the thickness of the films: (a) BFO-2- 150 nm, (b) BFO-4- 300 nm, (c) BFO-6- 450 nm, and (d) BFO-8 600 nm.

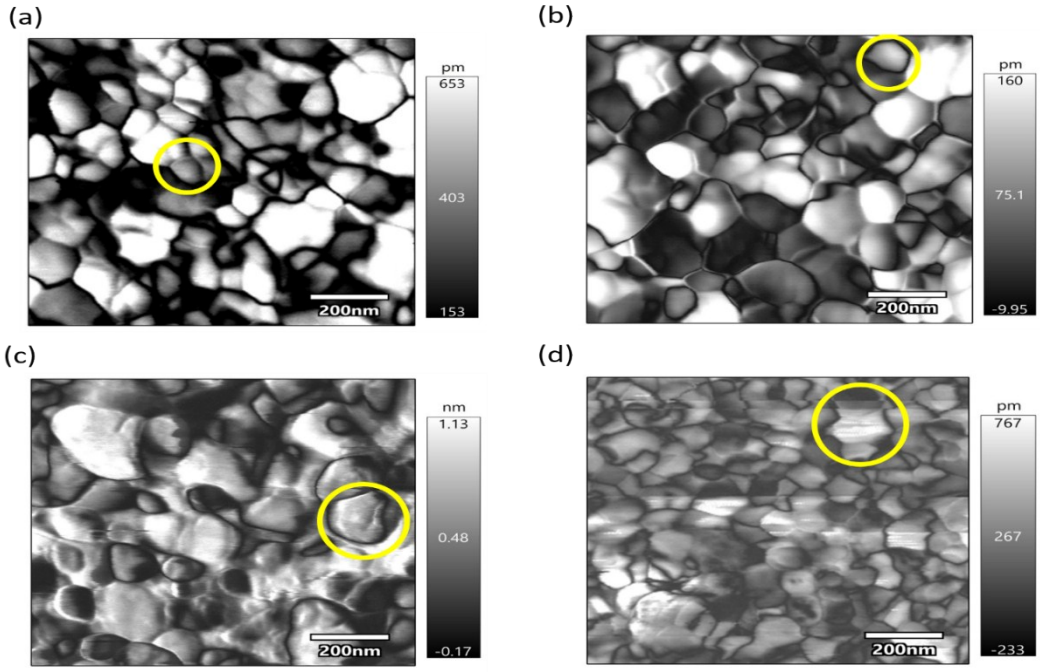

Fig. S5 Point poling results showing the domain size for all samples: (a) BFO-2, (b) BFO-4, (c) BFO-6, and (d) BFO-8, indicating the growth of domain with the increase of the film

thickness (Circles indicating the points where external bias was applied to study the domains switching phenomena).

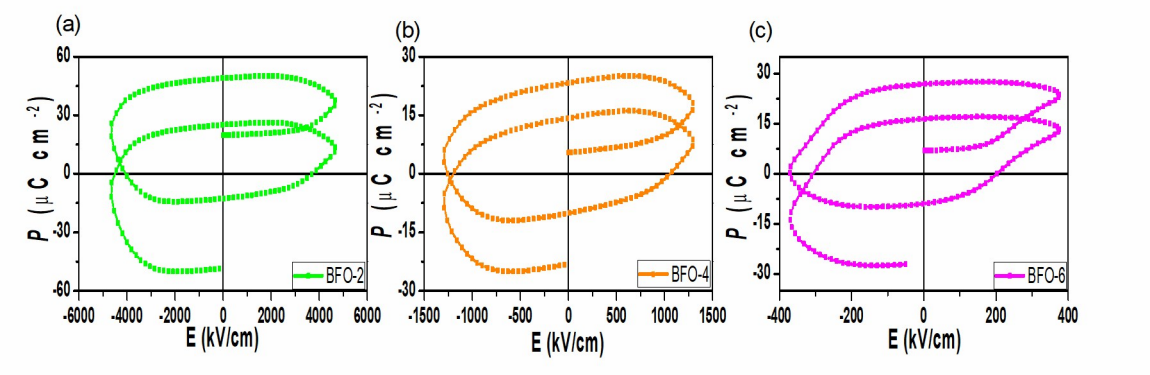

Fig. S6 P-E hysteresis loops for all samples: (a) BFO-2, (b) BFO-4, and (c) BFO-6. Compared with BFO-8, these samples show serious leakage phenomena and the real coercive fields and residual polarization cannot be obtained from the current P-E Loop.

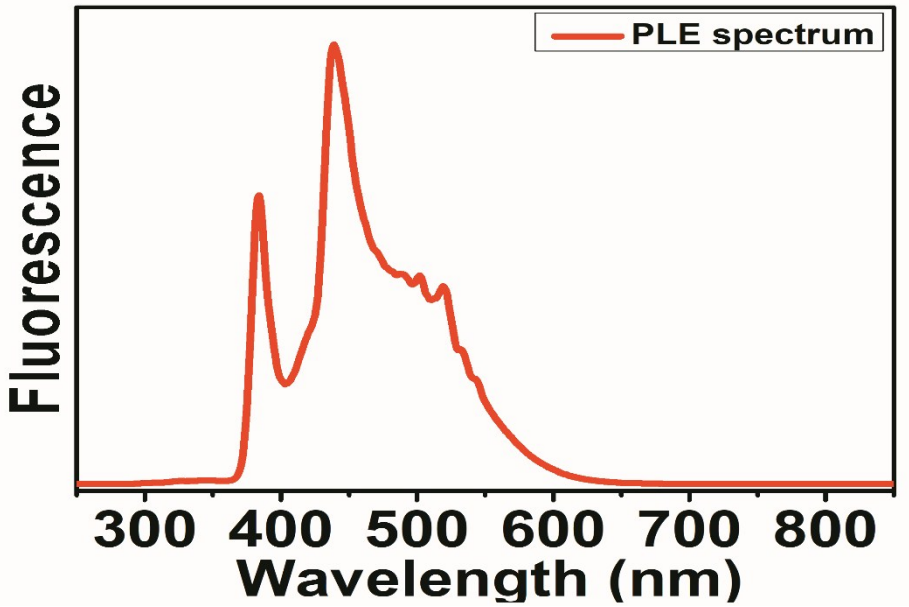

Fig. S7 Photoluminescence emission (PLE) spectrum of BFO-8 thin film without polarization. The sample was stored in a desiccator for 3 months.

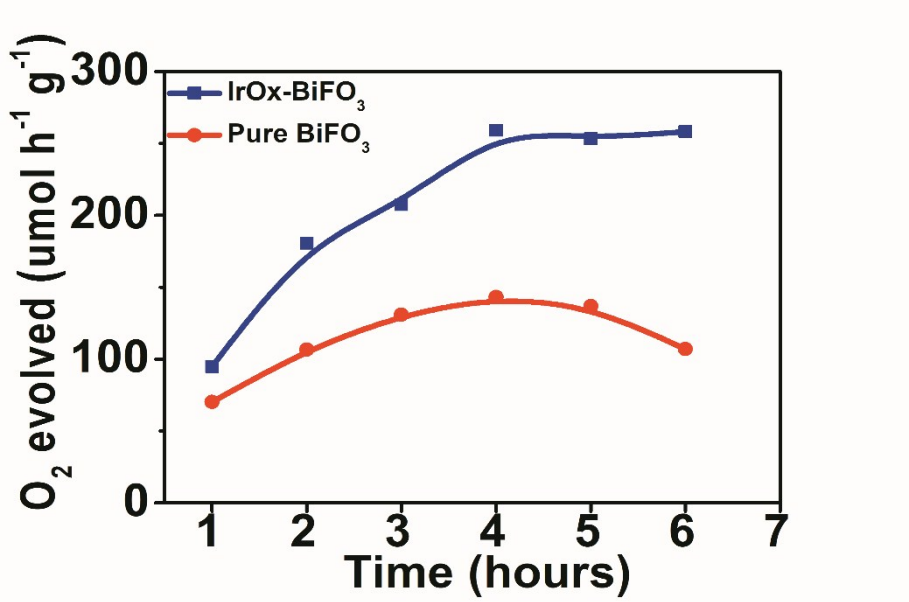

Fig. S8 Time courses of photocatalytic water oxidation on particulate pure BFO and IrO_x loaded BFO under visible light irradiation using sodium persulfate as the sacrificial reagent (pH =13).